INTERNATIONAL JOURNAL OF GEOMAGNETISM AND AERONOMY
VOL. 3, NO. 3, PAGES 281–287, FEBRUARY 2003

Lower stratosphere response to electric field pulse

N. V. Smirnova, A. N. Lyakhov, and S. I. Kozlov

Institute of Geosphere Dynamics, Moscow, Russia

Abstract. An improved plasmochemical model is developed to study the impact of electric field perturbations on the lower stratosphere aeronomy. It is shown that for any plasmochemical atmospheric model the critical electric field should be determined in the framework of the accepted atmosphere composition, electron impact ionization and electron attachment rates. The electron attachment taken into account as well as the complex negative ion chemistry modifies the threshold significantly. The requirements for accurate self-consistent initial data setting are given. Variations of negative ions, excited minor and long-lived neutral constituents are presented. Some aspects of applications to the blue jet event are discussed.

1. Introduction

Thunderstorm specific optical events referred to as blue jets, red sprites, and elves were intensively studied during last years. The experimental data available give the following characteristic heights and durations: blue jets, 15–40 km with the mean duration of about 200 ms; red sprites, 40–90 km with the mean duration of about 60 μs [*Sentman and Wescot*, 1995]. According to a number of observations such events occur during thunderstorms with the frequencies varied from 1/20 to 1/40 for the positive cloud-to-ground (CGD) discharges and from 1/200 to 1/400 for negative CGD. A number of theoretical models have been proposed up to date [*Sentman and Wescot*, 1995], such as (1) fluorescence induced by optical pumping of the middle or upper atmospheric gas, (2) quasistatic dielectric breakdown between clouds and the higher atmosphere, (3) quasistatic heating and impact excitation of the air in the middle atmosphere, (4) cosmic ray triggered runaway breakdown, and (5) radio frequency breakdown by lightning electromagnetic pulse.

Initial efforts to understand sprites and jets focused mainly on their relationship to causal electrical processes in thunderstorms. Therefore these models, except the one by *Mishin* [1997], do not include the complex system of photochemical and ionization/recombination processes in lower stratosphere, though the latter determine the response of the medium to any perturbations mentioned above.

Our opinion is that the calculation of optical emissions of blue jets must be preceded by detailed simulation of variations of minor neutral, excited, and charged constituents of the medium under the transition of electromagnetic pulses. Only as a result of such a simulation possible candidates for the certain band emissions can be determined exactly from the set proposed previously *Sentman and Wescot* [1995]. Concerning the realistic thunderstorm scenario, none of the treatments mentioned above takes into account the change of the chemical composition of the atmosphere caused by the preceding discharges.

We use the plasmochemical model which takes into account the realistic chemical composition of minor neutral, excited and ionized constituents as well as all types of processes discussed below. The critical value of the electric field required for the electron avalanche occurrence is determined self-consistently in the framework of the model itself. This allows us to determine precisely variations in the ionized and excited constituents. Moreover, based on a new evidence, we consider in this model the processes with negative ions involved. Their role was underestimated in the previous treatments. We present the comparison of the simulation results of the quasistatic electric field impact on the lower stratosphere with earlier theoretical estimates [*Mishin*, 1997] and discuss the possible blue jet applications.

Copyright 2003 by the American Geophysical Union.

Paper number GAI99323.
CCC: 1524–4423/2003/0303–0323$18.00

The online version of this paper was published 17 February 2003.
URL: http://ijga.agu.org/v03/gai99323/gai99323.htm
Print companion issued February 2003.

Table 1. Improved Rate Constants

Reaction	Rate Constant	Condition
$e + N_2 \rightarrow e + N_2(A^3\Sigma_u^+)$	$10^{-8.4-17.11/\theta}$	$2 \le \theta \le 10$
	$10^{-8.67-14.41/\theta}$	$10 < \theta < 100$
$e + N_2 \rightarrow e + N_2(B^3\Pi_g)$	$10^{-7.91-16.81/\theta}$	$2 \le \theta \le 10$
	$10^{-8.2-13.92/\theta}$	$10 < \theta < 100$
$e + N_2 \rightarrow e + N_2(a^1\Pi_g)$	$10^{-8.17-18.74/\theta}$	$3 \le \theta \le 10$
	$10^{-8.29-17.53/\theta}$	$10 < \theta < 100$
$e + N_2 \rightarrow e + N_2(C^3\Pi_u)$	$10^{-7.88-23.32/\theta}$	$4 \le \theta \le 20$
	$10^{-8.08-19.37/\theta}$	$20 < \theta < 100$
$e + O_2 \rightarrow e + O_2(a^1\Delta_g)$	$10^{-10.26-0.79/\theta}$	$2 \le \theta \le 4.5$
	$10^{-8.74-7.68/\theta}$	$4.5 < \theta \le 20$
	$10^{-8.68-7.7/\theta-0.0031\theta}$	$20 < \theta < 100$
$e + O_2 \rightarrow e + O_2(b^1\Sigma_g^+)$	$10^{-12.06+3.9710^{-2}\theta^2}$	$2 \le \theta \le 5$
	$10^{-9.13-9.7/\theta}$	$5 < \theta \le 10$
	$10^{-9.4-7.05/\theta-1.7\times10^{-3}\theta}$	$10 < \theta < 100$
$e + O_2 \rightarrow e + O + O$	$10^{-7.78-14.08}$	$3 \le \theta \le 10$
	$10^{-8.31-8.78/\theta}$	$10 < \theta \le 30$
$e + O_2 \rightarrow O^- + O$	$10^{-9.42-12.7/\theta}$	$3 \le \theta \le 9$
	$10^{-10.21-5.7/\theta}$	$9 < \theta \le 30$
$e + O_2 \rightarrow e + e + O_2^+$	$10^{-8.31-28.57/\theta}$	$6 \le \theta \le 26$
	$10^{-7.54-48.57/\theta+\log(1+410^{-7}\theta^3)}$	$26 < \theta < 100$
$e + N_2 \rightarrow e + e + N_2^+$	$10^{-8.09-40.29/\theta}$	$8 \le \theta \le 30$
	$10^{-7.37-61.81/\theta}$	$30 < \theta < 100$
$e + O_2 \rightarrow e + O(^3P) + O(^1D)$	$10^{-7.43-17.06/\theta}$	$3 \le \theta \le 10$
	$10^{-7.6-15.43/\theta}$	$10 < \theta \le 100$
$O_2^- + O_2 \rightarrow e + 2O_2$	$6.6 \times 10^{-19} \exp(0.94\theta)$	$\theta < 3$
	$10^{-10.15-36/\theta+28.9/\theta^{1.5}}$	$3 \le \theta$
$e + O_2 + O_2 \rightarrow O_2^- + O_2$	$(4.7 - \theta/4)10^{-31}$	
$e + O_2 + N_2 \rightarrow O_2^- + N_2$	$(4.7 - \theta/4)10^{-31}$	
$e + NO \rightarrow NO^+ + 2e$	$10^{-7.6-13.5/\theta}$	
$e + O_3 \rightarrow O^- + O_2$	$1.41 \times 10^{-8}\theta/300$	

2. Plasmochemical Model

We proceed with the plasmochemical model, developed previously for detailed studies of the aeronomy of the atmosphere during a microwave discharge [*Borisov et al.*, 1993]. Originally, the model includes 166 processes for the following 33 constituents: $O(^3P)$, $O_2(^1\Delta_g)$, O_3, H, OH, H_2O, HO_2, H_2, H_2O_2, $N(^4S)$, NO, N_2O, NO_2, $O_2(b^1\Sigma_g^+)$, $N(^2D)$, $N_2(C^3\Pi_u)$, $N_2(B^3\Pi_g)$, $N_2(a'^1\Sigma_u^-)$, $N_2(A^3\Sigma_u^+)$, O_2^+, N_2^+, NO^+, O_4^+, $O_2^+ \cdot H_2O$, $NO^+ \cdot N_2$, $NO^+ \cdot CO_2$, H_3O^+, $H_3O^+ \cdot$ OH, O_2^-, CO_3^-, O^-, NO_3^-, and electrons.

This model includes the processes of dissociation, dissociative ionization, ionization, excitation, electron attachment, dissociative attachment, detachment, dissociative recombination of positive ions with electrons, and various ion-molecular reactions of positive and negative ions, thus providing simulation in a wide height range (from 20 to 90 km). It also allows us to calculate a large number of excited constituents and optical emissions in a wide spectrum (UV–IR) as well as density variations of long-lived minor neutral constituents, the latter being especially important in the case of a sequence of perturbations and for the relaxation analysis.

The distinguishing feature of the model is that the set of equations for the chemical kinetics is closed on the initial conditions and a set of realistic self-consistent ambient densities of minor neutral and charged constituents. For this purposes the model includes the well-known processes of photodissociation of O_2, O_3, H_2O, H_2O_2, NO, NO_2, and N_2O as well as ionization of the atmosphere by cosmic rays and of NO and $O_2(^1\Delta_g)$ by the solar radiation.

We use the self-consistent method of solution of such set of chemical kinetic equations presented by *Kozlov et al.* [1982]. This method provides: (1) self-consistence of n_j in the framework of given chemical kinetics set of equations; (2) correct calculation of the atmospheric response to certain

Table 2. Additional Reactions

Reaction	Rate Constant
$O_2^+ + e \rightarrow O(^1D) + O(^3P)$	$3.87 \times 10^{-8}(1/\theta)$
$h\nu + \begin{pmatrix} O_2 \\ O_3 \\ N_2O \end{pmatrix} \rightarrow O(^1D) + \begin{pmatrix} O(^3P) \\ O_2(^1\Delta_g) \\ N_2 \end{pmatrix}$	J_i †
$N_2(A^3\Sigma_u^+) + O_2 \rightarrow N_2 + O(^3P) + O(^1D)$	2.8×10^{-11}
$N_2(B^3\Pi_g) + O_2 \rightarrow N_2 + O(^3P) + O(^1D)$	3×10^{-10}
$O(^1S) \rightarrow O(^1D) + h\nu$	$1.35\ s^{-1}$
$O(^1S) + O(^3P) \rightarrow O(^1D) + O(^1D)$	$5 \times 10^{-11} \exp(-301/T)$
$N_2(A^3\Sigma_u^+) + O(^1D) \rightarrow NO + N(^2D)$	7×10^{-12}
$O(^1D) + N_2 \rightarrow O(^3P) + N_2$	$2 \times 10^{-11} \exp(107/T)$
$O(^1D) + O_2 \rightarrow O(^3P) + O_2$	$2.9 \times 10^{-12} \exp(67/T)$
$O(^1D) + O_2 \rightarrow O(^3P) + O_2(b^1\Sigma_g^+)$	$2.6 \times 10^{-11} \exp(67/T)$
$O(^1D) + O_3 \rightarrow \begin{pmatrix} 2O(^3P) + O_2 \\ O_2 + O_2 \end{pmatrix}$	2.65×10^{-10}
$O(^1D) + H_2O \rightarrow OH + OH$	3.5×10^{-10}
$O(^1D) + H_2 \rightarrow OH + H$	2.9×10^{-10}
$O(^1D) + N_2O \rightarrow NO + NO$	1.1×10^{-10}
$O(^1D) \rightarrow O(^3P) + h\nu$	9.9×10^{-3}
$N_2(A^3\Sigma_u^+) + O(^3P) \rightarrow O(^1S) + N_2$	2.8×10^{-11}
$O(^3P) + O(^3P) + O(^3P) \rightarrow O(^1S) + O_2$	2×10^{-32}
$O_2(A^3\Sigma_u^+) + O(^3P) \rightarrow O_2 + O(^1S)$	4.5×10^{-11}
$O(^1S) + O(^1S) \rightarrow e + O_2^+$	3×10^{-11}
$O(^1S) + N(^4S) \rightarrow e + NO^+$	3×10^{-11}
$O(^1S) + O(^3P) \rightarrow O(^1D) + O(^1D)$	$5 \times 10^{-11} \exp(-301/T)$
$O(^1S) + O_2 \rightarrow O(^3P) + O_2$	$4.9 \times 10^{-12} \exp(-860/T)$
$O(^1S) \rightarrow O(^1D) + h\nu$	$1.35\ s^{-1}$
$O_2 + e \rightarrow O_2(A^3\Sigma_u^+) + e$	$10^{-7.9-13.4/\theta}$
$O(^3P) + O(^3P) + M \rightarrow O_2(A^3\Sigma_u^+) + M$	4.7×10^{-34}
$O_2(A^3\Sigma_u^+) + N_2 \rightarrow O_2 + N_2$	9.3×10^{-15}
$O_2(A^3\Sigma_u^+) + O_2 \rightarrow O_2 + O_2$	2.9×10^{-13}
$O_2(A^3\Sigma_u^+) + O \rightarrow O_2 + O(^1S)$	4.5×10^{-11}
$O_2(A^3\Sigma_u^+) \rightarrow O_2 + h\nu$	$5\ s^{-1}$

† The rates for these processes are specific for certain simulation parameters

perturbation; (3) correct definition of the perturbed initial conditions for the subsequent disturbance; and (4) determination of long-term aftereffects of the electric field impact on the stratosphere and mesosphere, in particular variations in the principal long-lived components (NO, O_3) with their further influence on the charged components.

The plasmochemical model discussed above was significantly upgraded according to the modern experimental and theoretical data. First of all, it was done for the rates of the reactions with electrons and negative ions, especially important for the correct description of the processes at low altitudes. The rates modified according to *Alexandrov and Napartovich* [1993], *Alexandrov et al.* [1995], and *Massey* [1976] are presented in Table 1. For the purpose of emission calculations the processes of excited constituents production $O(^1D)$, $O(^1S)$, and $O_2(A^3\Sigma_u^+)$ were also included. The reaction list is presented in Table 2 [*Brasseur and Solomon*, 1984; *Popov*, 1994]. It was found that these modifications change qualitatively and significantly the results of simulation. The main restriction to the model is the requirement that the atmosphere under consideration must stay "cool" during a sequence of perturbations.

Initial equilibrium densities of the most important nitrogen and oxygen constituents (in cm^{-3}) at 20 km for the daytime conditions are $[O(^3P)] = 9.4 \times 10^5$, $[O_3] = 3 \times 10^{12}$, $[O_2(^1\Delta_g)] = 10^{10}$, $[O_2(b^1\Sigma_b^+)] = 10^4$, $[O(^1D)] = 2.5$, [NO]= 3×10^8, and $[N(^4S)] = 7 \times 10^2$. The initial densities at 30 km are $[O(^3P)] = 6.1 \times 10^5$, $[O_3] = 4.5 \times 10^{12}$, $[O_2(^1\Delta_g)] = 1.1 \times 10^{10}$, $[O_2(b^1\Sigma_b^+)] = 1.8 \times 10^5$, $[O(^1D)] = 50$, [NO]= 10^9, and $[N(^4S)] = 7 \times 10^2$.

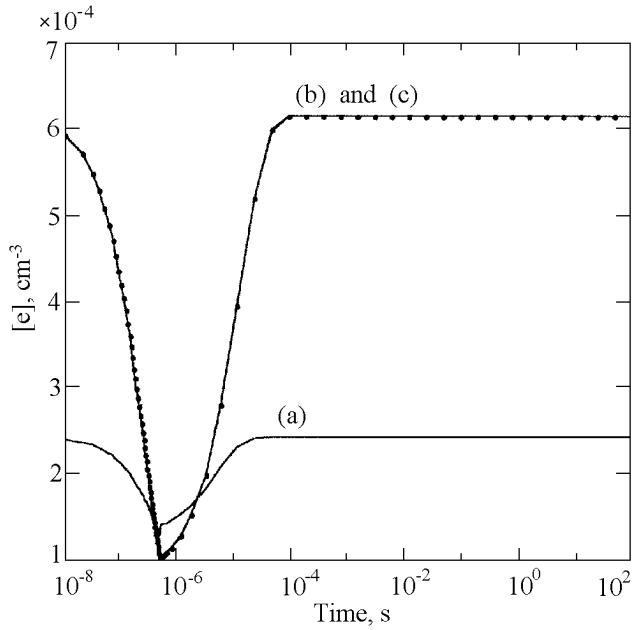

Figure 1. Variations of the electron density at 20 km. Indices correspond to the rates from *Borisov et al.* [1993] (curve a), the modified rates from Table 1 (curve b), and the processes listed in Table 2 (curve c).

The following equilibrium densities of the charged components at 20 km were obtained in the steady state simulation: $[e] = 6.2 \times 10^{-4}$, the positive ion density $[N_+] \approx 6.3 \times 10^3$, the negative ion density $[N_-] \approx [N_+]$. Corresponding values at 30 km are $[e] = 2.5 \times 10^{-3}$ and $[N_+] = [N_-] \approx 5.7 \times 10^3$. In the negative ion composition the major ions are NO_3^- and CO_3^-, and in the positive ion composition the major ions are H_3O^+ and $H_3O^+ \cdot OH$.

3. Critical Electric Field

The determination of the critical electric field which provides the occurrence of an avalanche was described by *Bazelyan and Raizer* [1997]. As a result of theoretical analysis and solution of the Boltzman equation for electrons, the following condition is obtained and widely used: $\theta = 10^{16} E/N_m$, where E is the electric field in V cm^{-1} and N_m is the number density in cm^{-3}. For the critical electric field $\theta \approx 12$. In the previous work on atmosphere perturbation by blue jets [*Mishin*, 1997], a different scaling law is used: $E_{cr} \approx 40\tilde{p}$ kV m^{-1}, where $\tilde{p}$ is the atmospheric pressure normalized to that at 30 km [see also *Papadopolous et al.*, 1993]. We determine the critical value based on the usual physical rule that the critical electric field provides an equivalence of the ionization ν_i and attachment plus recombination $\nu_a + \nu_r$ frequencies.

The fact should be noted specially that the atmosphere reaction to an electric field pulse depends on whether is it below or above the electron avalanche appearance threshold. This corroborates the necessity of "self-determination" of E_{cr} in the study of the atmosphere response to electric field variations especially at low heights, which are of interest for the blue jet problem.

The threshold values obtained in theoretical models and within a model itself may vary significantly. For example, at heights of 20 and 30 km our values of the critical electric field are 1995.9 V cm^{-1} and 427 V cm^{-1} respectively, instead of 1600 V cm^{-1} and 400 V cm^{-1} of *Mishin* [1997] and 2160 V cm^{-1} and 468 V cm^{-1} of *Bazelyan and Raizer* [1997]. One can see that at lower heights, where the main role in electron loss is played by their attachment to the electronegative gases, the difference is quite large (up to 500 V cm^{-1}). The importance of a redetermination of the critical electric field can be seen from the following results. We performed a numerical simulation of the atmospheric response to an electric field pulse with the magnitude and duration taken from *Mishin* [1997] ($\tau_p = 2/\tilde{p}$, $E_{20} = 1600$ V cm^{-1}, and $E_{30} = 400$ V cm^{-1}) with the self-consistent steady-state initial conditions under the ambient electric field value of 1.93 V cm^{-1}. The summer daytime conditions were assumed. The electron density variations due to propagation of the first electric field pulse are shown in Figures 1 and 2 for the heights of 20 and 30 km, respectively. The values of E indicated are well below the real critical electric field, so no avalanche process is observed. A decrease of the electron density occurs (instead of its growing) because the attachment frequency increases with the electric field faster than the ionization frequency. This continues until the electric field reaches the critical value. One can see from the data presented how importance it is to use correct rate con-

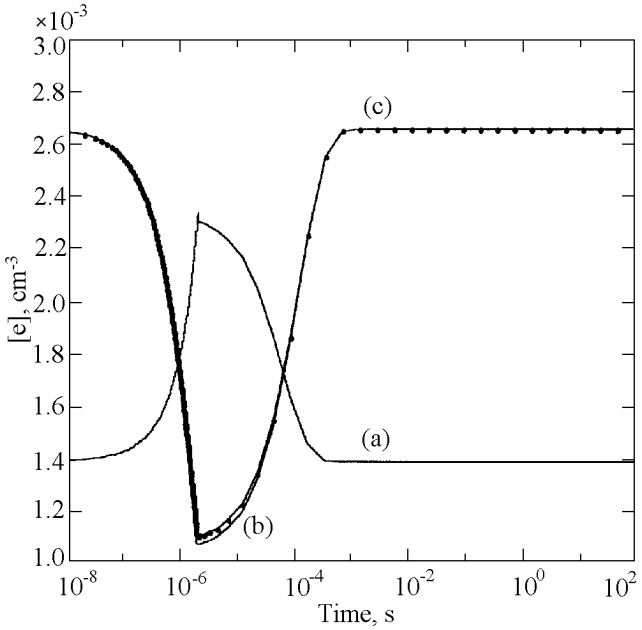

Figure 2. Variations of the electron density at 30 km Indices correspond to the rates from *Borisov et al.* [1993] (curve a), the modified rates from Table 1 (curve b), and the processes listed in Table 2 (curve c).

stants. At 30 km the use of the old rates [*Borisov et al.*, 1993] provides a small increase of the electron density and simultaneously production of the minor excited constituents responsible for the blue emissions observed.

The correct usage of the rate constants together with the self-consistent initial data show no significant disturbance in the middle atmosphere under the critical electric field calculated according to *Mishin* [1997]. The setting of the initial electron density equal to $10^7\tilde{p}^2$ cm^{-3} used by *Mishin* [1997] is not self-consistent, and so its usage makes the simulation results unreliable (it is worth noting that the reaction set used by *Mishin* [1997] is not closed and even in such a system some rates were taken erroneously though being referenced to *Borisov et al.* [1993]).

4. Lower Stratosphere Response to Large Electric Field

We determined the electric field required for the production of $10^7\tilde{p}^2$ cm^{-3} electrons during the pulse time. The latter was chosen according to *Mishin* [1997]: $\tau_p = 2/\tilde{p}$ μs. Such production rate is obtained under $E = 2871$ V cm^{-1} = $1.44E_{cr}$ at 20 km and under $E = 616.5$ V cm^{-1} = $1.45E_{cr}$ at 30 km.

In such a case the simulation shows a rapid increase of $[e]$ during the pulse and a prolonged decay after it. The latter effect is caused by the significant growth of $[O(^3P)]$ (Figure 3) which leads to a modification of the negative ion composition (from the NO_3^- ions dominating in the ambient atmosphere to CO_3^- ions and to the initial ions O_2^- and O^-) and, thus to an increased electron detachment (Figure 4).

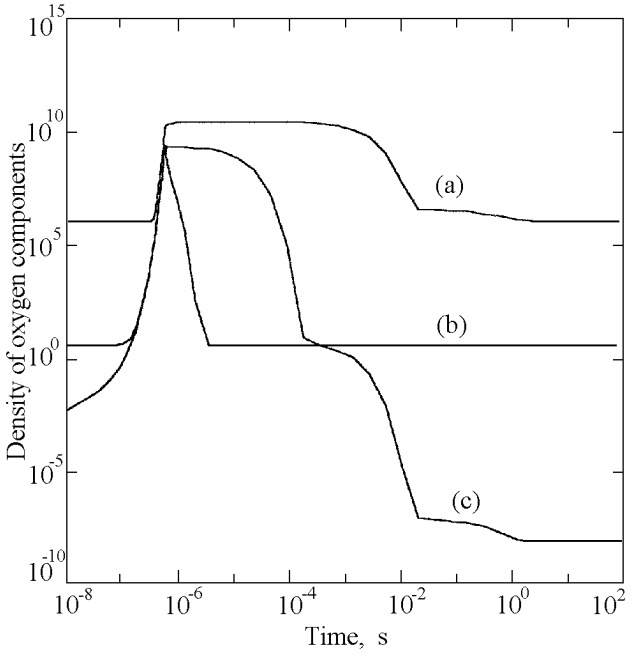

Figure 3. Variations of some oxygen components at 20 km during a strong field pulse propagation: $O(^3P)$ (curve a), $O(^1D)$ (curve b), and $O_2(A^3\Sigma_u^+)$ (curve c).

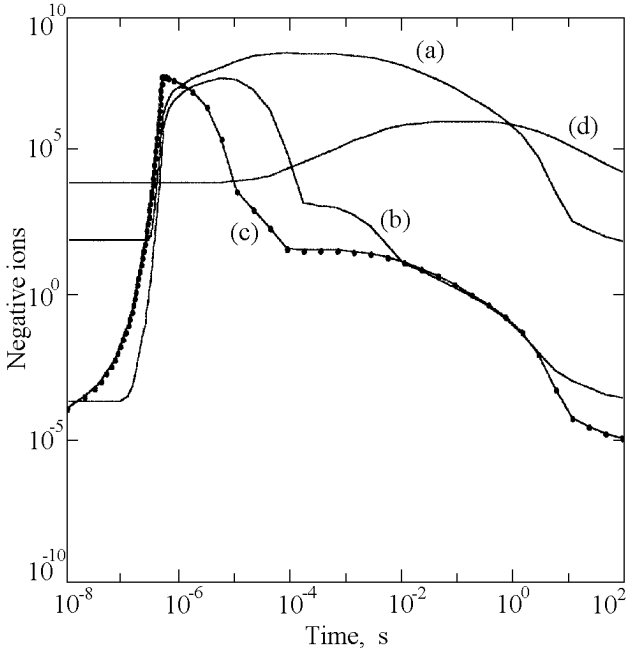

Figure 4. The negative ion composition at 20 km: CO_3^- (curve a), O_2^- (curve b), O^- (curve c), and NO_3^- (curve d).

Figures 5 and 6 show the relative density variations $\delta X = (X(t) - X_0)/X_0$ of the most important long-lived components in the stratosphere. The ozone density is characterized by an increase of $[O_3]$ (up to 0.9% at $h = 20$ km and $\approx 0.035\%$ at $h = 30$ km), which occurs at the stage of the

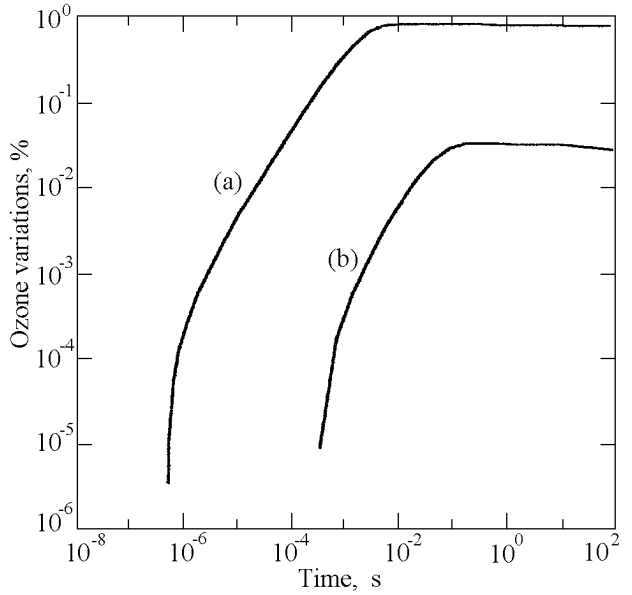

Figure 5. The ozone variations at 20 km (curve a) and at 30 km (curve b).

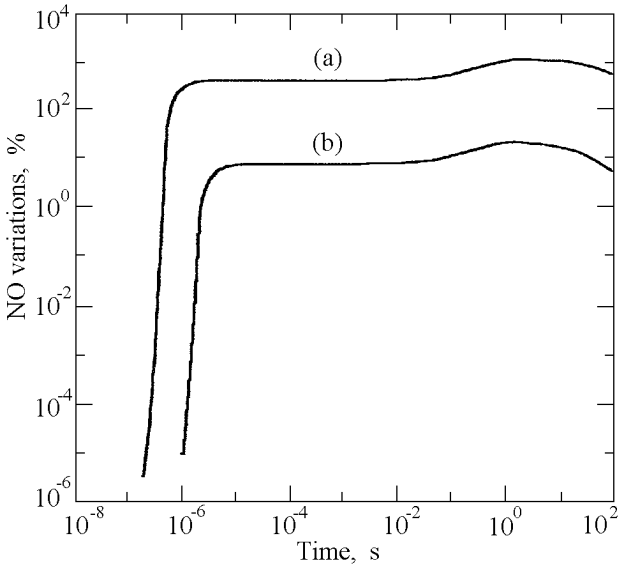

Figure 6. The nitric oxide variations at 20 km (curve a) and at 30 km (curve b).

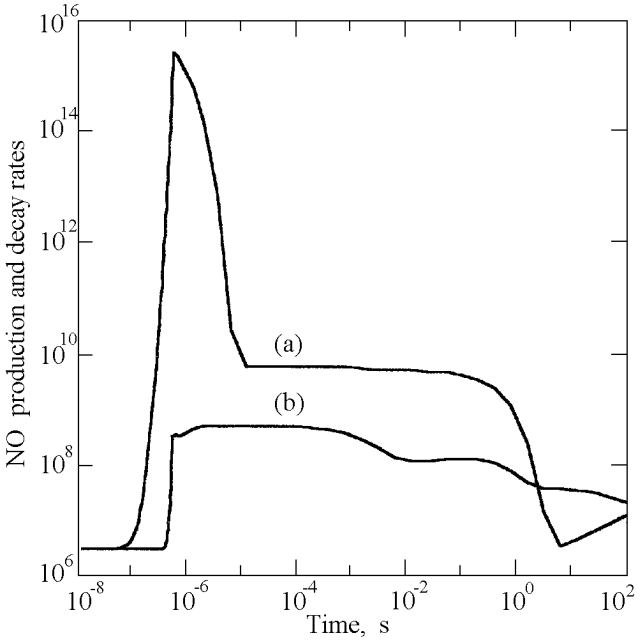

Figure 7. The total NO production (curve a) and decay (curve b) rates at 20 km.

perturbed atmosphere relaxation. The latter is a result of the $[O(^3P)]$ increase under O_2 dissociation in collisions with electrons.

The NO behavior (Figure 6) seems unusual, with a slight increase of δNO after the pulse. Then there us a plato till 10^{-3} s and a further fast growth up to $\delta NO = 1120\%$ at $h = 20$ km and $\approx 18\%$ at $h = 30$ km at $t = 1 - 2$ s. Then [NO] decreases slowly; however, it does not relax down to the ambient value at least till 100 s.

To explain such [NO] behavior, one should compare Figure 7, where the total rates of NO production (curve a) and decay (curve b) are presented, with Figure 8, where the variations of nitrogen compounds $N(^2D)$, $N(^4S)$, and $N_2(A^3\Sigma_u^+)$ are shown (both data refer to 20 km). The initial growth of [NO] is determined by its production in the following processes:

$$N(^2D) + O_2 \rightarrow NO + O \quad (1)$$

$$N_2(A^3\Sigma_u^+) + N_2O \rightarrow NO+ \quad (2)$$

$$N(^4S) + N_2 \quad (3)$$

$$N(^4S) + O_3 \rightarrow NO + O_2 \quad (4)$$

$$O(^1D) + N_2O \rightarrow NO + NO \quad (5)$$

It is worth noting that the inclusion of the processes with excited constituents $O(^1D)$, $O(^1S)$, $O_2(A^3\Sigma_u^+)$ increases the NO production by 4 times as compared with the simulation performed without these components. The "plato" of [NO] in Figure 6 continuing till $t \approx 10^{-3}$ s is caused by almost stationary $[N(^4S)]$ and $[O(^3P)]$ which provide approximately constant rates of NO production and disappearance. Further increase of [NO] at $t > 10^{-3}$ s is due to a decrease of the rate of the decay processes in three-body collisions $(NO+O(^3P) + N_2 \rightarrow NO_2 + O(^3P))$ with almost the same production rate resulted from the high $N(^4S)$ density. Finally, the decrease of $N(^4S)$, as a source of NO, at $t > 1-2$ s with the constant loss rate, leads to a decrease of [NO]. The variations described in the long-lived components O_3 and NO differ significantly from the results of *Mishin* [1997] for the same values of $[e]$ and τ_p. First of all, it is true for the

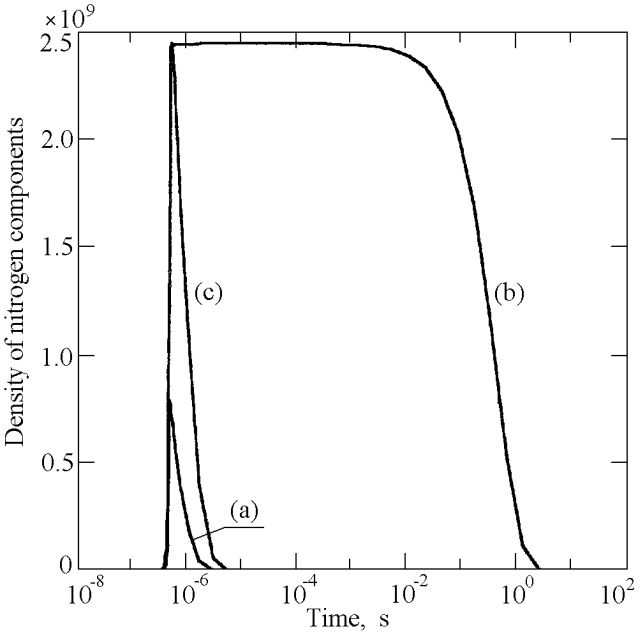

Figure 8. Variations of some nitrogen components at 20 km: $N(^2D)$ (curve a), $N^4S)$ (curve b), and $N_2(A^3\Sigma_u^+)$ (curve c).

significantly smaller variations of δO_3 (by a factor of 15 at $h = 30$ km and a factor of 50 at $h = 20$ km) and for the larger δNO (by a factor of 1.8) at $h = 30$ km in our simulation, with δNO at 20 km corresponding well to the *Mishin* [1997] results. The altitude dependence of the maximum δX values differs, though the tendency of the effect to increase at lower heights is clearly detected in both models. The above mentioned differences demonstrate the necessity of (1) a precise and full inclusion of the processes that establish the ambient distribution of long-lived components as well as their variations under electromagnetic pulse propagation, and (2) a use of the initial densities obtained self-consistently in the framework of the chemical kinetics reaction set assumed.

5. Discussion

In the blue jet models developed up to the date, the major complexity arises from the problem of the initial ionization, required for avalanche occurrence. According to *Sukhorukov and Stubbe* [1998] an initial preparation of the medium at the electric field $E = 0.3E_{cr}$ is needed, which is significantly larger than the one in the ambient atmosphere. In the *Pasko et al.* [1996] model the occurrence of an electron avalanche is due to the ignoring of electron disappearance in the attachment processes.

In this work we have shown that (1) in the case of precise calculation of the ionization level in the ambient atmosphere together with detailed inclusion of all processes governing the electron density at the heights specific for blue jets, the threshold of an avalanche increase of the electron density is not reached, under thunderstorm originated electromagnetic field pulse magnitudes; and (2) the magnitude of E_{cr} required for the avalanche and emission occurrence should be determined based on correct dependencies of the ionization and attachment rates on the electric field magnitude with realistic atmosphere composition taken into account.

An accurate consideration of blue jets requires a self-consistent calculation of the variations of ionized, excited and minor neutral constituents during the electric field pulse propagation as well as during the relaxation stage, thus taking into account the medium variations under transition of consequent pulses and the perturbation accumulation effects.

In conclusion, we note that the results presented allow us to assume that a possible candidate for the emissions in the blue spectral range at $h = 15 - 40$ km (blue jets) may be $O_2(A^3\Sigma_u^+)$ ($\lambda = 260 - 380$ nm), since (as one can see from the comparison of Figures 3 and 8) $N_2(A^3\Sigma_u^+)$ and $O_2(A^3\Sigma_u^+)$ have almost the same densities ($10^8 - 10^9$ cm^{-3} at $h = 20 - 30$ km) but the life-time of the latter is much longer.

Acknowledgments. This work was partially sponsored by the Russian Foundation for Basic Research (project 00-05-64146). We thank I. V. Nemchinov for useful discussions.

References

Alexandrov, N. L., and A. P. Napartovich, Processes in gases and plasma with negative ions, *Usp. Fiz. Nauk (in Russian), 163*, 1, 1993.

Alexandrov, N. A., N. A. Dyatko, and I. V. Kochetov, Rate of nonelastic electron processes in the partially ionized plasma in a nonstationary electric field, *Fiz. Plasm. (in Russian), 21*, 806, 1995.

Bazelyan, E. M., and Yu. P. Raizer, *Spark Discharge,* CRC Press, Boca Raton, Fl., 1997.

Borisov, N., S. Kozlov, and N. Smirnova, Changes in the chemical composition of the middle atmosphere during multiple microwave pulse discharge in the air, *Kosmich. Issled. (in Russian), 31*, 177, 1993.

Brasseur, G., and S. Solomon, *Aeronomy of the Middle Atmosphere,* 441 pp., D. Reidel, Hingham, Mass., 1984.

Kozlov, S. I., V. A. Vlaskov, and N. V. Smirnova, Ion kinetics, minor neutrals and excited constituents in the D region when the ionization level is enhanced, I, Posing the problem and the overall scheme of the processes, *Kosmich. Issled. (in Russian), 20*, 624, 1982.

Massey, H., *Negative Ions,* Cambridge Univ. Press, New York, 1976.

Mishin, E., Ozone layer perturbation by a single blue jet, *Geophys. Res. Lett., 24,* 1919, 1997.

Papadopolous, K., G. Milikh, A. Gurevich, A. Drobot, and R. Shanny, Ionization rates for atmospheric and ionospheric breakdown, *J. Geophys. Res., 98*, 17,593, 1993.

Pasko, V. P., U. S. Inan, and T. F. Bell, Blue jets produced by quasi-electrostatic pre-discharge thundercloud fields, *Geophys. Res. Lett., 23,* 301, 1996.

Popov, N. A., Simulation of plasmochemical processes initiated by a powerful UHF discharge in the air, *Fiz. Plasm. (in Russian), 20*, 109, 1994.

Sentman, D. D., and E. M. Wescot, Red sprites and blue jets: Thunderstorm-excited optical emissions in the stratosphere, mesosphere, and ionosphere, *Phys. Plasmas, 39,* 2514, 1995.

Sukhorukov, A., and P. Stubbe, Problems of the blue jet theory, *J. Atmos. Terr. Phys., 60,* 725, 1998.

S. I. Kozlov, A. N. Lyakhov, and N. V. Smirnova, Institute of Geosphere Dynamics, Moscow, Russia.
(alyakhov@idg.chph.ras.ru; nsmirnova@idg.chph.ras.ru)

(Received 1 November 1999; revised 17 December 2002;
accepted 27 December 2002)